

**ON THE DOPPLER FREQUENCY SHIFTS OF RADAR SIGNALS
BACKSCATTERED FROM THE SEA SURFACE****S. A. Ermakov,^{1,2,3,4} * I. A. Kapustin,^{1,2,3}
V. N. Kudryavtsev,² I. A. Sergievskaya,^{1,2,3}
O. V. Shomina,^{1,2,3} B. Chapron,² and
Yu. Yu. Yurovskiy⁵**

UDC 551.466

We study the frequency spectra of the radar signals scattered from the wind waves on the sea surface in the full-scale experiment. Two types of the radar Doppler shifts of the spectrum maximum, namely, the averaged shift of the instantaneous spectrum of the scattered signal and the shift of the maximum of the signal time-averaged spectrum as functions of the incidence angle and the wind velocity and direction are analyzed for different sounding-wave polarizations. Significant difference between the average shift of the instantaneous spectrum and the shift of the average-spectrum maximum is demonstrated. This difference is attributed to the radar-signal modulation effect in the field of long surface waves. The obtained results are very important for correct retrieval of the velocities of the surface currents using the data of the satellite-borne measurements of the radar Doppler shifts.

1. INTRODUCTION

Microwave radars, in particular satellite-borne radars are widely used for solving the problems of remote ocean sounding when studying the oceanic and atmospheric processes by their manifestations on the sea surface (e.g., see [1–4] and references therein). The satellite-borne synthetic aperture radars, which have recently been employed for measuring the sea-current velocities using information on the radar Doppler shifts, are at present most widely used. For example, using the data of the “Envisat” synthetic aperture radar the Doppler shifts are analyzed, their experimental dependences on the observation conditions and the wind velocity are developed for various radio-wave polarizations, and empirical expressions for retrieving the current velocities are proposed in [5, 6]. A number of interesting features observed in the Doppler-shift experiment, including their substantial difference for the vertical and horizontal polarizations, are described in [6]. However, the physical mechanisms determining these features have not been studied comprehensively.

Physical substantiation of the algorithms for retrieving the surface-current velocities from the characteristics of the surface-scattered radar signal requires detailed analysis and improvement of the existing electromagnetic-wave scattering models. With respect to the Doppler shifts, the problem is reduced to the issue of the scattering-element velocity on the wavy water surface. This issue is fairly nontrivial and related to the scattering-mechanism features.

* stas.ermakov@hydro.appl.sci-nnov.ru

¹ Institute of Applied Physics of the Russian Academy of Sciences, Nizhny Novgorod; ² Russian State Hydrometeorological University, St. Petersburg; ³ N. I. Lobachevsky State University of Nizhny Novgorod; ⁴ Volga State Academy of Water Transport, Nizhny Novgorod; ⁵ Marine Hydrophysical Institute, Sevastopol, Russia. Translated from *Izvestiya Vysshikh Uchebnykh Zavedenii, Radiofizika*, Vol. 57, No. 4, pp. 267–280, April 2014. Original article submitted November 13, 2013; accepted February 5, 2014.

In the Bragg scattering model and the two-scale model (e.g., see [7, 8]), which is the generalization of the former, the scatterer velocity is the phase velocity of the surface waves with resonant length. It should be noted that the resonance scattering waves can be both “free” waves, which propagate with the phase velocity of the gravity-capillary waves, and “driven” (parasitic) waves, which are excited due to nonlinearity by the longer waves and propagate with the velocity of these long carrier waves [9–16]. Note that the excitation mechanisms and the characteristics of the driven waves significantly depend on their wavelength and can substantially differ for different frequency bands of the sounding radar signals.

Under conditions of the quasi-mirror scattering from the long surface waves (Kirchhoff’s approximation; see [7, 8]), the scatterer velocity corresponds to the projection of the velocity of the mirror points (moving at the phase velocity of a long wave) onto the direction of the sounding-radiation wave vector.

Although the mechanism of scattering from the wave-breaking zones and, accordingly, the issue of the scatterer velocity in them have not been fully clarified, much attention is paid to the development of the corresponding scattering models in [17–19].

According to [20–22], analysis of the radar-signal modulation by the long waves is an important aspect of the problem of the radar Doppler shift. As is shown below, modulation can significantly influence this shift.

In the general case, the above-mentioned mechanisms act jointly, while the resulting Doppler shift is determined by their relative contribution to scattering. Therefore, to further determine the roles of various mechanisms and develop the scattering models, one should conduct special experimental studies of the characteristics of the radar signals, including their Doppler spectra, for various radio-wave polarizations, observation geometries, wind velocities, and the long-wave amplitudes on the sea surface.

This work is aimed at obtaining new data on the Doppler shifts in the X-band of the radio waves and estimating the influence of the modulation effects of the radar-signal intensity on the Doppler shifts.

2. EXPERIMENT AND DATA PROCESSING



Fig. 1. Oceanographic platform of the Marine Hydrophysical Institute.

The experiments were performed in September 2012 on the basis of the oceanographic platform of Marine Hydrophysical Institute (Fig. 1), which is located in the near-shore area of the Black Sea approximately 0.6 km from the shore. The sea depth near the platform is 30 m. The X-band coherent scatterometer was operated at a wavelength of 3.2 cm using the offset antenna with a directional-pattern width of about 5° . The scatterometer was mounted on the platform at a height of 12 m above the unperturbed water surface. The signal scattered from the sea surface was received with polarization (vertical or horizontal) which coincided with that of the radiated signal. During the experiments, polarization was varied by the antenna rotation by 90° around its axis. The sounding-wave incidence angle and the azimuthal observation angle with respect to the wind direction varied in the ranges 25° – 55° and 0° – 180° , respectively. The wind velocity and direction were measured by the WIND SONIC ultrasound anemometer mounted at a height of 15 m.

In the experimental series, the wind velocities varied in the interval 7–14 m/s, while the periods and the wavelengths of the energy-carrying wind waves were 3–5 s and 30–50 m, respectively. The linear size of the scatterometer-irradiated area on the water surface was 2–4 m depending on the incidence angle, i.e., about 0.1 of the wavelength of the energy-carrying waves which determined modulation of the radar-scattering intensity.

The instantaneous (current) Doppler spectrum $S(\omega, t)$ of the detected radar signal was calculated for times shorter than the long-wave period (during the calculations, the latter was assumed equal to 0.125 or 0.25 s). The Doppler shift $F_1(t)$, which corresponded to the current spectrum $S(\omega, t)$, i.e., the instantaneous-spectrum shift, was determined as location of the barycenter of the function $S(\omega, t)$ on the frequency axis (see the Appendix). The average shift of the instantaneous spectrum was obtained by averaging of the function $F_1(t)$ over the time about 10–15 min, i.e., the time significantly exceeding the energy-carrying wave period.

When calculating the average Doppler spectrum and the corresponding Doppler shift of the average spectrum, the spectrum averaging time was found in the course of the data processing. During the processing, it was determined that estimation of the Doppler shift of the averaged spectrum almost ceased to depend on time for the averaging times about and over 10 min. The fluctuations of the estimate of this quantity and, therefore, its estimation error were in the interval 1–2 Hz. Examples of the instantaneous and averaged Doppler spectra are shown in Fig. 2.

The modulation transfer function was calculated according to its definition (see the Appendix and, e.g., [20–22]). To find the Fourier components of the orbital velocity $U(\Omega)$ of the long surface waves, which modulated the radar-signal intensity, the time series of the instantaneous-spectrum shifts were used. In this case, it was naturally assumed that the average shift of the instantaneous spectrum is proportional to a certain constant velocity of the scatterers, while the variable part of the shift is proportional to the orbital-velocity amplitude (or the displacement amplitude linearly related to the orbital-velocity amplitude) of the long waves. The maximum of the spectrum of the instantaneous Doppler shift was located in the interval 0.2–0.35 Hz. However, since the coherence-function maximum (see the Appendix) was located at somewhat higher frequencies in the range 0.25–0.5 Hz (see Fig. 3), the amplitude and phase of the modulation transfer function $m(\Omega)$ were estimated at the frequencies of the coherence-function maximum. When finding the transfer function, the entire realization with a duration of about 10–15 min was divided into several segments (the number of the segments was much greater than unity) with durations significantly exceeding the long-wave period (in this case, 32 s).

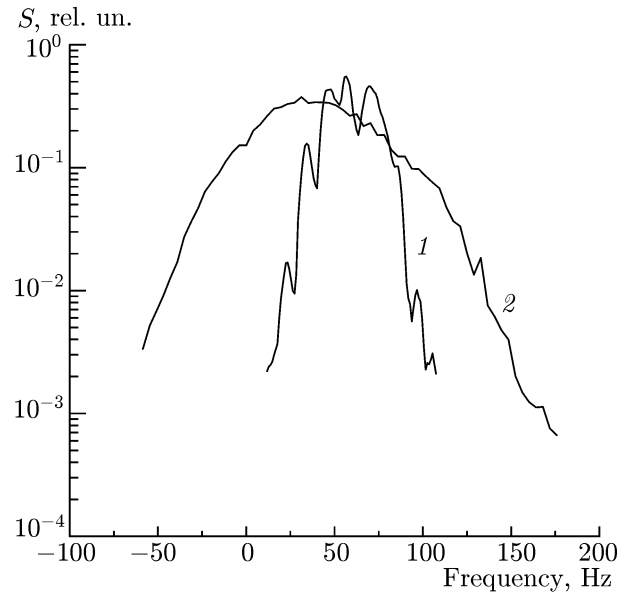


Fig. 2. Examples of the experimentally obtained Doppler spectra S of the reflected radar signal: instantaneous spectrum near the long-wave crest (curve 1) and the average spectrum (curve 2).

3. EXPERIMENTAL RESULTS

3.1. Doppler shifts

Let us consider the Doppler-shift dependences on the radio-wave incidence angle, which are experimentally obtained and are shown in Fig. 4.

The presented experimental dependences show that (a) the average Doppler shift of the instantaneous spectrum and the Doppler shift of the average spectrum increase with increasing incidence angle (b), the average Doppler shifts of the instantaneous spectra are smaller than the Doppler shifts of the average spectra for both downwind and upwind observations and (c), the average Doppler shifts of the instantaneous spectra have close values for both downwind and upwind observations, whereas the Doppler shifts of the average spectra for the upwind observations are greater than those for the downwind observations. In addition, the Doppler average, in particular the average Doppler shift of the instantaneous spectrum, comparatively

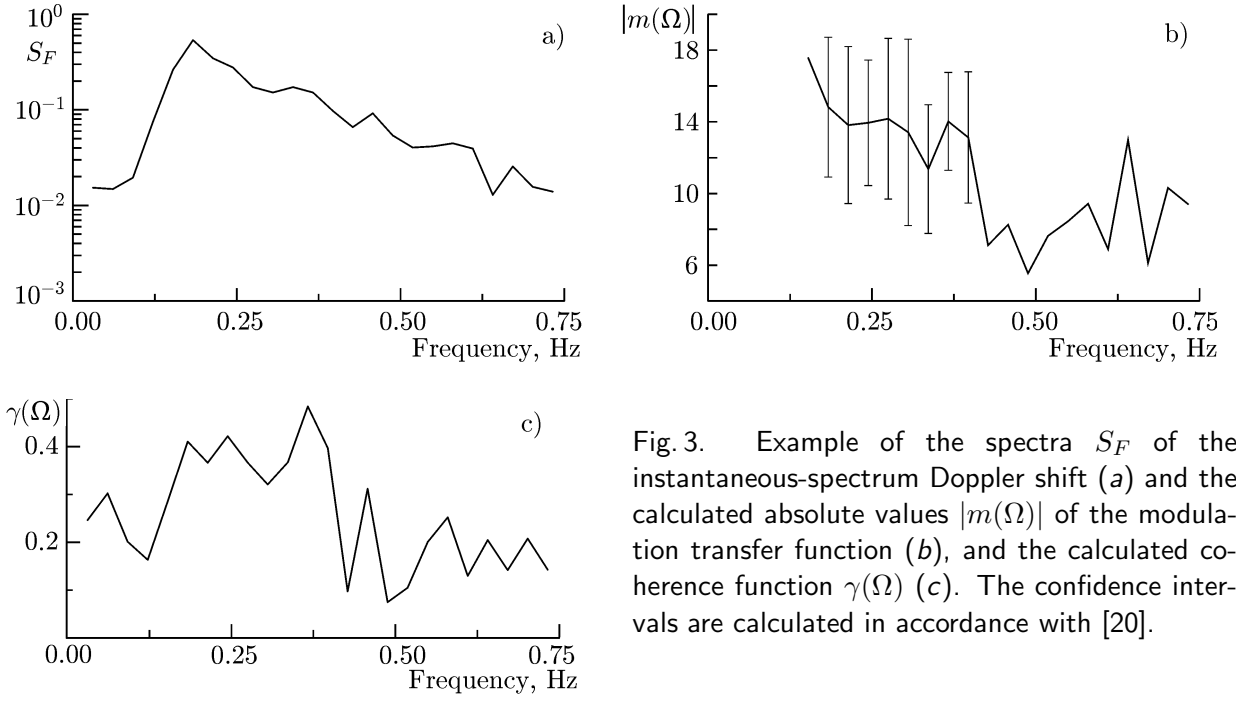


Fig. 3. Example of the spectra S_F of the instantaneous-spectrum Doppler shift (a) and the calculated absolute values $|m(\Omega)|$ of the modulation transfer function (b), and the calculated coherence function $\gamma(\Omega)$ (c). The confidence intervals are calculated in accordance with [20].

weakly depend on the wind velocity in the studied range of its values, which follows from a rather small shift spread for the wind velocities ranging from 7 to 14 m/s. Under such conditions, the contribution of the wind drift to the Doppler shift is small, which explains the weak dependence of the Doppler shift on the wind velocity.

3.2. Modulation transfer function

Analysis of modulation of the radar signals shows that the absolute value of the modulation transfer function depends on the wind velocity, the observation angle with respect to the wind direction, the incidence angle, and polarization of the sounding electromagnetic wave. The function falls off with increasing incidence angle and wind velocity. For the horizontal polarization, the absolute value of the modulation transfer function for the upwind observation is greater than that for the downwind observation. Modulation for the horizontal polarization turns out to be significantly (by 2–3 times) stronger than that for the vertical polarization. The phase of the modulation transfer function was equal to 0.5–1.5 and $-(0.5-1.5)$ for the upwind and downwind observations, respectively. On the whole, the experimentally obtained absolute values of the modulation transfer function agree with those given in the literature (e.g., see [20, 22]). Figure 5 shows its experimental values as functions of the incidence angle for the vertical and horizontal polarizations at the wind velocities 10–13 m/s.

3.3. Analysis and discussion of the results

The obtained data show that the average Doppler shifts of the instantaneous spectra are almost identical for both polarizations in the case of the upwind and downwind observations of the radar scattering.

For moderate incidence angles, the Bragg scattering mechanism, according to which the radar-signal power is determined by the spectral intensity of the surface waves with the resonance (Bragg) wavelength λ_B , satisfying the relationship

$$\lambda_B = \lambda_0 / (2 \sin \theta), \quad (1)$$

where λ_0 is the wavelength of the electromagnetic wave and θ is its incidence angle, is believed to be one of the main scattering mechanisms (see [7, 8]).

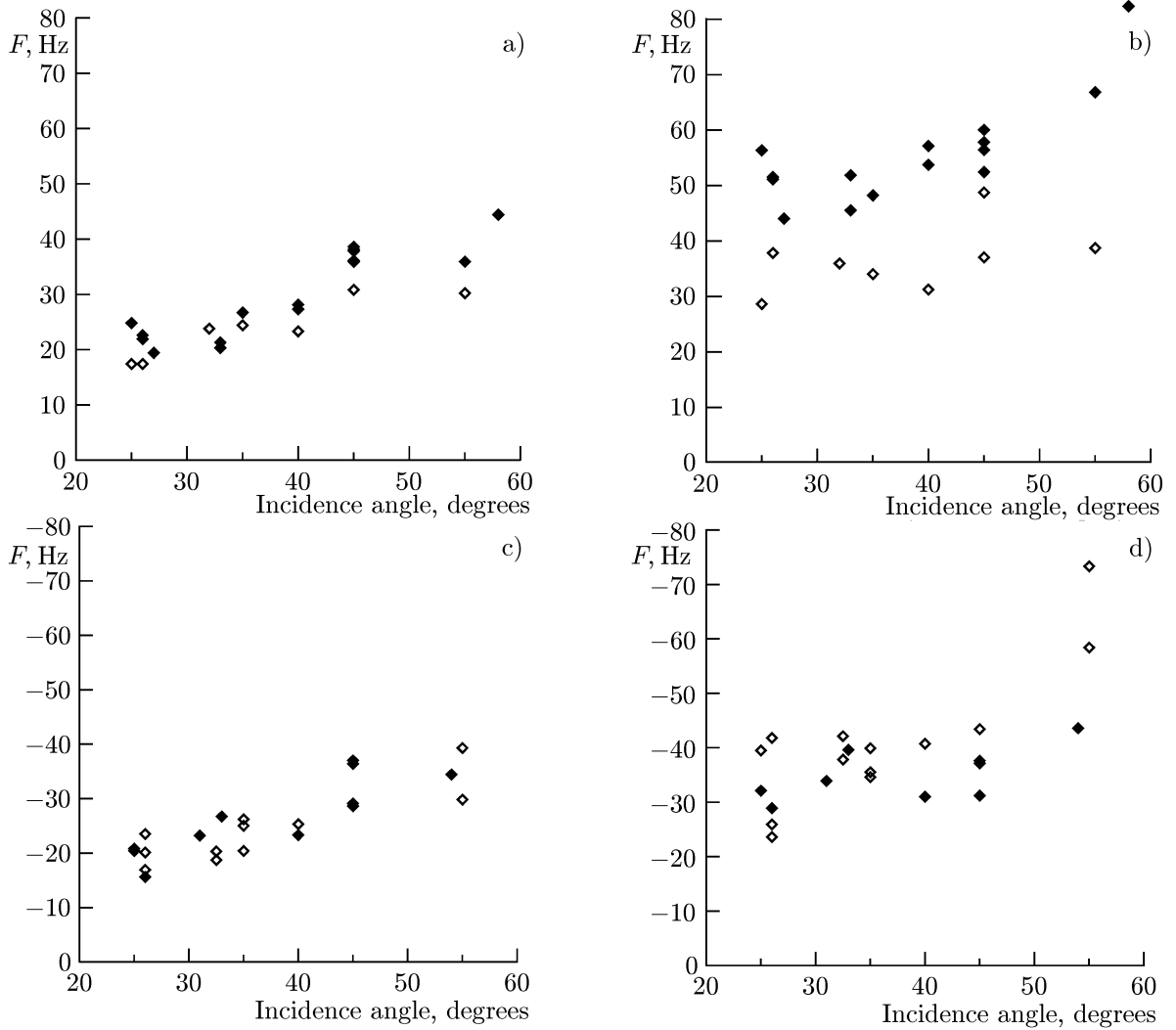


Fig. 4. Doppler shifts F as functions of the incidence angle for the upwind observation: averaged shift of the instantaneous spectrum of the scattered signal (a) and the shift of the maximum of the time-averaged signal spectrum (b). Black and white dots correspond to the horizontal and vertical polarizations of the radio waves, respectively. Panels c and d show the same as panels a and b, respectively, but for the downwind observation.

As was mentioned above, the Bragg waves can be both free, i.e., propagating with the velocities of the linear gravity-capillary waves, and driven, i.e., excited (due to nonlinearity) by longer waves and propagating with their velocities. Nonresonant scattering for which the emerging nonpolarized component of the scattered radiation is stipulated by the wave breaking, is also discussed in the literature [16–19, 23–25] along with the resonant (Bragg) mechanism. A significant role of the nonresonant mechanism in the radar-signal formation is supported, in particular, by the presence of short and intense peaks (bursts) in the signal-intensity dependence on time. In this case, the polarization ratio, i.e., the ratio of intensities of the signals with the vertical and horizontal polarizations, can approach unity for the moderate incidence angles (when the mirror-reflection mechanism is insignificant), i.e., be much smaller than the values predicted by the Bragg model. In some works (see, in particular, [3, 4, 26]), to describe the nonresonant component, it was proposed to allow for diffraction by the wedges whose role in this case is played by the sharpened crests of the waves which are longer and move with velocities greater than that of the free Bragg ripples. However, a detailed discussion of the nonresonant-component nature is beyond the scope of this work, which mainly focused on the difference between the Doppler shifts of the instantaneous and average spectra.

Theoretical dependence of the Doppler shifts of the instantaneous spectrum on the incidence angle

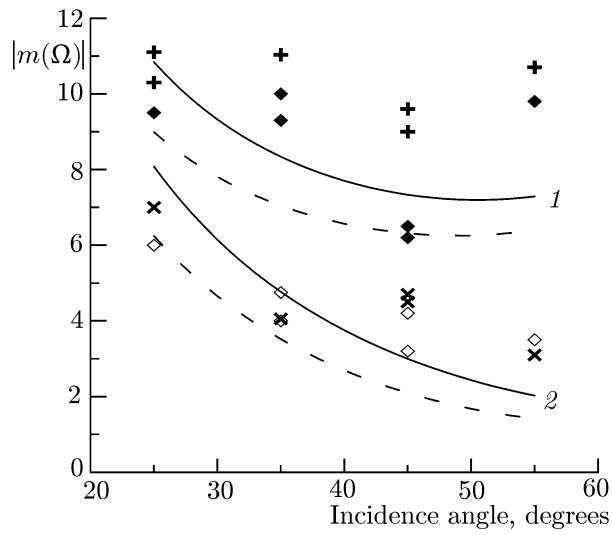


Fig. 5. Absolute value $|m(\Omega)|$ of the modulation transfer function as a function of the incidence angle at the wind velocities 10–13 m/s for the horizontal (upwind (+) and downwind (◆)) and vertical (upwind (×) and downwind (◇)) polarizations of the radio waves. Theoretical curves 1 and 2 correspond to the horizontal and vertical polarizations of the radio waves, respectively, dashed curves correspond to the downwind observations, and solid curves to the upwind observations.

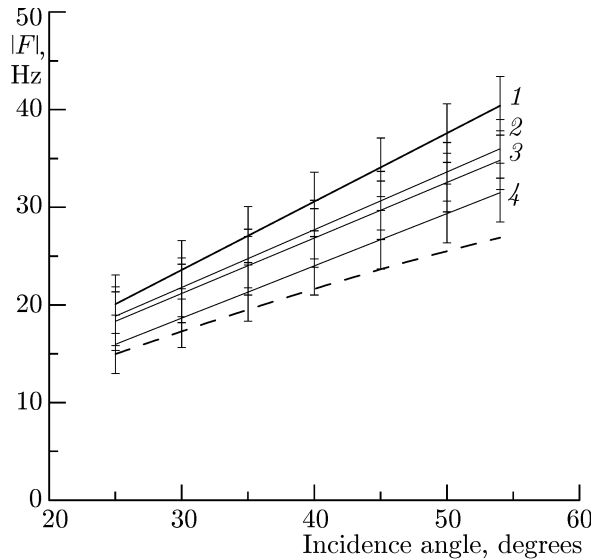


Fig. 6. Smoothed experimental dependences of the averaged Doppler shifts F of the instantaneous spectra for various radio-wave polarizations and observation conditions (curves 1 and 2 correspond to the horizontal polarization, and curves 3 and 4, to the vertical polarization for the downwind observations (curves 1 and 3), and the upwind observations (curves 2 and 4)) and the model dependence for the Bragg scattering from free ripples. For the upwind and downwind measurements, the shifts $F > 0$ and $F < 0$, respectively. The confidence interval is determined by the spread of the measured values.

for the Bragg component of scattering from free waves is shown in Fig. 6 (dashed curve) in which the experimentally obtained smoothed dependences of the average Doppler shifts of the instantaneous spectra are for comparison shown for two polarizations in the cases of downwind and upwind sounding. It can be concluded that the Bragg model yields the Doppler-shift values which are smaller than those experimentally obtained, but still sufficiently close to them (the case of the upwind horizontal polarization is an exception). Therefore, on the one hand, the non-Bragg component significantly contributes to the scattering intensity, whereas, on the other hand, the Doppler shifts of the radar signal are close to the values predicted by the Bragg model.

This seeming contradiction can be explained as follows. It is obvious from the experimental-data analysis, the nonresonant-scattering contribution is mainly concentrated in the strong signal bursts whose intensity significantly (by 5–10 times) exceeds the average intensity (see Fig. 7). Therefore, despite the short relative duration of the bursts (the total duration of the bursts is shorter than 0.1 of the realization duration), their energy is comparable to the average one. Thus, the share of the nonresonant scattering component is comparable to the Bragg one, which is responsible for the significant difference of the polarization ratio from that predicted by the Bragg model. The Doppler shifts in the bursts usually exceed the realization-average values, but this excess is insignificant (about two times; see Fig. 7). With allowance for a small duration of the bursts, their Doppler shifts weakly influence the resulting Doppler shift and, therefore, its value is comparable to the estimates yielded by the Bragg model.

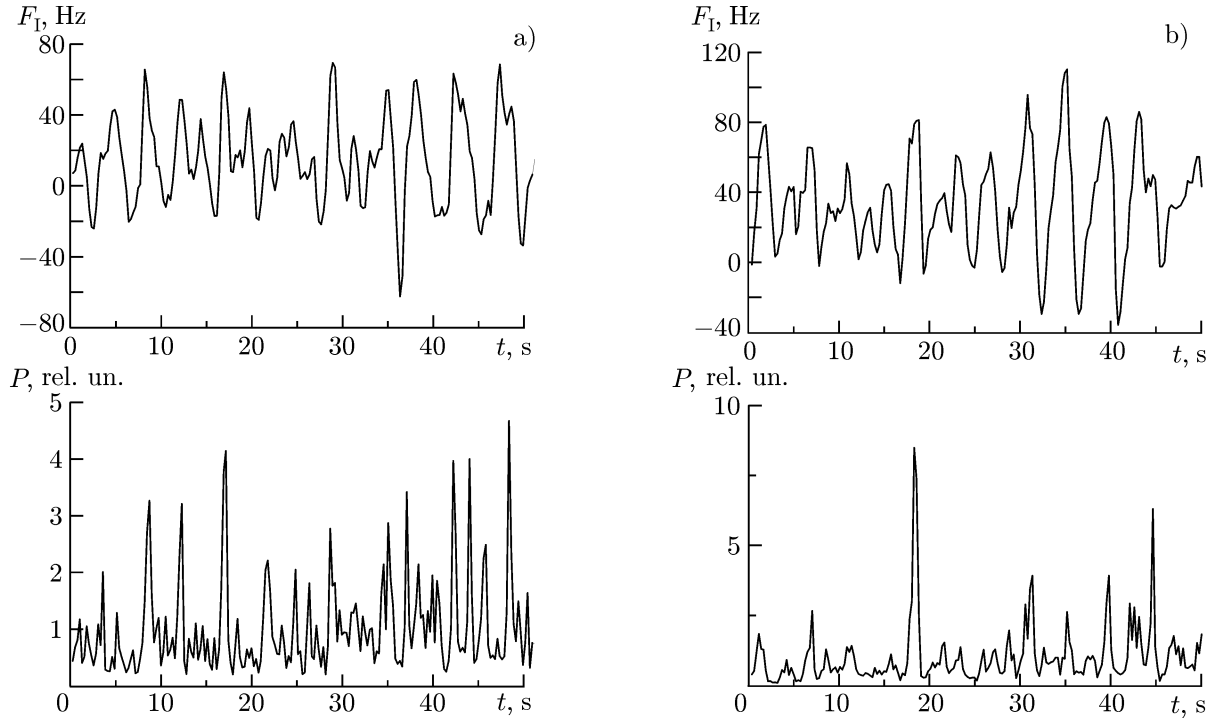


Fig. 7. Examples of realizations of the Doppler shift $F_I(t)$ of the instantaneous spectrum and the signal intensity $P(t)$ normalized to its average value for the vertical (a) and horizontal (b) polarizations.

When sounding by the centimeter-range radar, the driven Bragg waves have the wavelengths about several centimeters and can be the harmonics of the longer, decimeter, surface waves. In this case, the Doppler shift increases since the phase velocity of the decimeter waves and their harmonics is greater than that of free resonant ripples. However, for correct allowance for this effect, one should have the data on the measured characteristics of the decimeter waves and the amplitudes of their higher harmonics. The estimate of the Doppler shift of the instantaneous spectrum also increases due to the nonzero diameter of the radar-irradiated sea-surface region. Strictly speaking, we experimentally determine the Doppler shift of the spectrum averaged over the radar spot, rather than the instantaneous-spectrum shift. Therefore, the Bragg ripples modulation by the waves with the wavelengths shorter than the spot diameter additionally contributes to the average Doppler shift of the instantaneous spectrum in the same manner how the radar-signal modulation by the waves that are long compared with the spot size stipulates the difference between the Doppler shifts of the instantaneous and average spectra (see the discussion below).

Let us analyze the cause of the difference between the Doppler shifts of the average and instantaneous spectra. As is shown in the Appendix, the difference between the average Doppler shift of the instantaneous spectrum and the shift of the average spectrum is determined by the modulation transfer function. Let us estimate its absolute value within the framework of the well-known model with allowance for the geometric- and hydrodynamic-modulation effects.

For simplicity, we consider one-dimensional surface waves. According to [20–22] the modulation transfer function, which determines geometric modulation, has the form

$$m_g(\Omega) = i \tanh(\kappa H) \left[\frac{1}{R_p} \frac{dR_p}{d\theta} + \tan \theta + \cot \theta \frac{d \ln F(k_B)}{d \ln k_B} \right] + \frac{2 \tanh(\kappa H)}{\kappa h}, \quad (2)$$

where R_p is the radar scattering coefficient for the waves with a given polarization, (see, e.g., [2, 20]), $F(k_B)$ is the wind-wave spectral density for the Bragg wave number k_B , h is the radar height above the sea surface, and H is the water depth. Equation (2) describes the geometric modulation of the radar-signal intensity because of the variations in the distance to the scattering region (due to the water-surface displacement

by a long wave) and variations in the radar-scattering coefficient, the wave number, and the intensity of scattering Bragg ripples (caused by the variations in the local incidence angle, which is determined by the long-wave tilt).

The expression for the hydrodynamic modulation of the Bragg ripples by the variable orbital currents in a long wave has the form (see, e.g., [21, 22])

$$m_h(\Omega) = -\frac{d \ln N(k_B)}{dk_B} \left(1 - \frac{c_g}{C} - \frac{i\beta_r}{\Omega} \right)^{-1}, \quad (3)$$

where $N(k_B) = F(k_B)/\omega(k_B)$, $\omega(k) = \sqrt{gk + \sigma k^3/\rho}$ is the gravity-capillary wave frequency, β_r is the Bragg wind-ripple relaxation parameter determined as the difference between the wind-excitation and viscous-damping coefficients, c_g is the ripple group velocity, and C is the long-wave phase velocity. In the calculations, the derivative $-d \ln F(k_B)/d \ln k_B$ was assumed equal to four, the wind-excitation coefficient was obtained from the well-known empirical expression given in [27] for the wind velocity 10 m/s, and the long-wave frequency was assumed equal to 0.25 Hz. The results of calculations of the function $|m(\Omega)|$ are given in Fig. 5 under the downwind and upwind observation conditions with allowance for the hydrodynamic and geometric components. The figure also presents the absolute value of the geometric modulation transfer function (dashed line), which is the same for the downwind and upwind sounding. Therefore, we can conclude that within the framework of this model, geometric modulation dominates over the hydrodynamic one under the experimental conditions. The theoretical curves in Fig. 6 qualitatively agree with the experimental results.

Let us estimate the theoretical difference between the Doppler shift of the average spectrum and the average Doppler shift of the instantaneous spectrum using the performed model calculations of the modulation transfer function. Such estimates based on Eq. (A11) in the Appendix are shown in Fig. 8. Calculations allowed for the modulation at the energy-carrying wave frequencies near the coherence-function maximum. The generally satisfactory agreement of the estimates and the experimental results allows one to conclude that the radar-signal modulation in the presence of the long wind waves explains the main features of the differences between the average Doppler shifts of the instantaneous spectra and the Doppler shifts of the average spectra, as well as the features of the average-spectrum shifts for different polarizations. Note that the discrepancy between theoretical and experimental results, which is observed in Fig. 8 for significant incidence angles (55° in our experiment), can be related to an increase in the contribution of nonresonant scatterers to the scattering with increasing incidence angle (see [26]).

4. CONCLUSIONS

Thus, the full-scale studies of the Doppler shifts of the X-band radar signal were performed for different polarizations, radiation-incidence angles, and wind velocities and directions. It has been shown that the averaged shift of the instantaneous spectrum increases with increasing incidence angle, relatively weakly depends on the wind velocity and direction, and has close values for the vertical and horizontal polarizations. The Doppler shift satisfactorily agrees with the estimates based on the Bragg scattering model even in the presence of strongly nonlinear (breaking) waves.

In turn, the Doppler shift of the average spectrum exceeds the averaged shift of the instantaneous spectra and is different for the vertical and horizontal polarizations, as well as for the upwind and downwind sounding. The features of the Doppler shifts of the average spectrum are satisfactorily explained by the influence of the radar-signal intensity modulation in the field of the long wind waves.

The obtained results are important for correct estimation of the current velocity from the Doppler shift measurements, in particular those performed by the satellite-borne radars. In fact, the resolution elements in the sea-surface images usually amount to tens of meters (synthetic aperture radars ERS-1, ERS-2, and “Envisat”) for the satellite-borne synthetic aperture radars, whereas they can be much larger for the radars with conventional (nonsynthetic) aperture. Therefore, the Doppler shifts estimated from

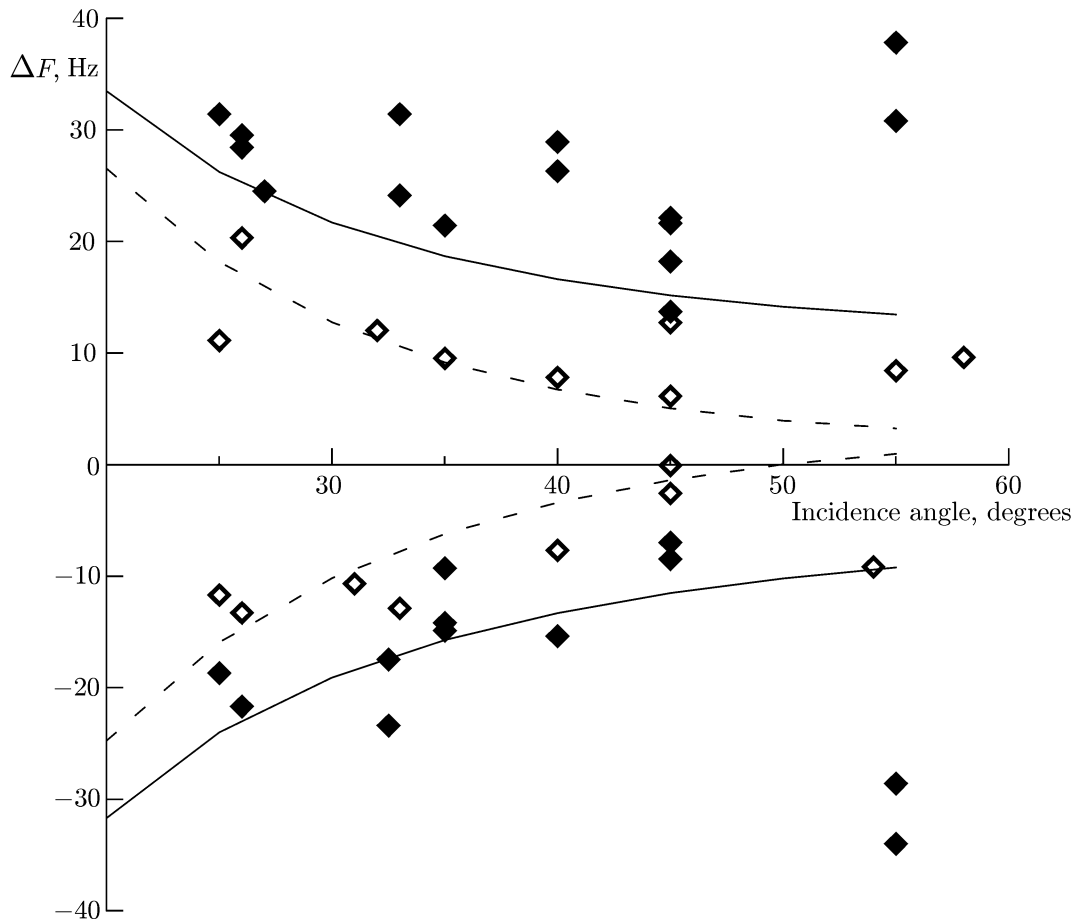


Fig. 8. The difference ΔF between the Doppler shifts of the average spectra and the average Doppler shifts of the instantaneous spectra as a function of the incidence angle for the upwind (positive values of ΔF) and downwind (negative values of ΔF) observations. Black and white symbols correspond to the horizontal and vertical polarizations of the sounding radio waves, respectively. Theoretical calculations are shown by the solid and dashed lines for the horizontal and vertical polarizations, respectively.

the radar-sounding data contain the component that is determined by the radar-signal modulation by the wind waves whose wavelengths are shorter than the sizes of the resolution element, i.e., actually are the Doppler shifts of the average spectrum (in this case, the fact that this spectrum is space-averaged rather than time-averaged is insignificant). Incorrect allowance for this component can overestimate the current velocity retrieved from the Doppler shift measurements.

We thank V. V. Bakhanov for interest in our studies and valuable comments.

This work was supported by the Russian Foundation for Basic Research (project Nos. 11-05-00295, 13-05-90429-Ukr_f_a, 13-05-97058, 13-05-97043, and 14-05-00876), the Russian Academy of Sciences (project “Radiophysics”), the State Foundation for Basic Research of Ukraine (project No. F53/117-2013 of 04.06.2013), and the Government of the Russian Federation (project No. 11.G34.31.0078).

APPENDIX

DOPPLER FREQUENCY SHIFTS AND THE MODULATION TRANSFER FUNCTION OF THE RADAR SIGNAL

Basic definitions

Let $S(\omega, t)$ be the instantaneous (current) spectrum of the radar signal, which is analyzed at the times that are short compared with the characteristic periods of the modulating long waves. Then the Doppler shift of the instantaneous spectrum can be defined as

$$F_I(t) = \frac{1}{2\pi} \int_0^\infty S(\omega, t) \omega \, d\omega \bigg/ \int_0^\infty S(\omega, t) \, d\omega. \quad (\text{A1})$$

The Doppler shift F_A of the average spectrum of the radar signal is defined in accordance with the expression

$$F_A(t) = \frac{1}{2\pi} \int_0^\infty \omega \bar{S}(\omega, t) \, d\omega \bigg/ \int_0^\infty \bar{S}(\omega, t) \, d\omega, \quad (\text{A2})$$

where the spectrum

$$\bar{S}(\omega, t) = \frac{1}{T} \int_{-T/2}^{+T/2} S(\omega, t) \, dt \quad (\text{A3})$$

is obtained as the average value over the time $T \gg 2\pi/\Omega$, which is significantly larger than the characteristic periods $2\pi/\Omega$ of the long (energy-carrying) wind waves.

The definition of the modulation transfer function is based on representing the intensity of a radar signal reflected from the sea surface as

$$P(t) = \bar{P} \left[1 + \int m(\Omega) \frac{U(\Omega)}{C(\Omega)} \exp(i\Omega t) \, d\Omega \right] + P_r, \quad (\text{A4})$$

where $U(\Omega)$ and $C(\Omega)$ are the Fourier components of the horizontal orbital and phase velocities of the long waves at the frequency Ω , \bar{P} is the average intensity of the radar signal, and P_r is the fluctuating part of the radar signal, which is uncorrelated with the long wave. In this case, the modulation transfer function $m(\Omega)$ is written in the form

$$m(\Omega) = \frac{C(\Omega)}{\bar{P}} \frac{\overline{P(\Omega)U^*(\Omega)}}{|U(\Omega)|^2}, \quad (\text{A5a})$$

where the asterisk “*” denotes complex conjugation. When finding the function $m(\Omega)$ from the radar-measurement data, it is assumed (see [20–22]) that the Doppler shift variations of the radar signal are determined by the orbital velocities of the modulating long waves, so that instead Eq. (A5a) we can write

$$m(\Omega) = k_e \frac{C(\Omega)}{\pi \bar{P}} \frac{\overline{P(\Omega)F_I^*(\Omega)}}{|F_I(\Omega)|^2} \exp(-i\theta), \quad (\text{A5b})$$

where $k_e = 2\pi/\lambda_0$ and λ_0 is the electromagnetic wavelength. The coherence function

$$\gamma^2(\Omega) = \frac{|\overline{P(\Omega)U^*(\Omega)}|^2}{|\overline{P(\Omega)}|^2 |\overline{U(\Omega)}|^2}, \quad (\text{A6})$$

which represents the correlation degree of the radar-signal fluctuations with the long wave, is also an im-

portant characteristic when analyzing the radar-signal modulation. In Eqs. (A5a), (A5b), and (A6), the quantity $P(\Omega)$ is the Fourier component of the radar-signal power and the overbar denotes averaging over the ensemble (time).

Relationship between the Doppler frequency shifts and the modulation transfer function of the radar signal

The definition of the instantaneous (current) spectrum of the radar signal yields

$$S(\omega, t) = \frac{1}{2\pi} \int \overline{\text{Re}[A(t) \exp[i\varphi(t)] \text{Re}[A(t + \tau) \exp[i\varphi(t + \tau)]] \exp(i\omega t)} \, d\tau, \quad (\text{A7})$$

where $A(t)$ and $\varphi(t) = 2k_e r(t)$ are the amplitude and phase of the backscattered electromagnetic wave, respectively, and $\mathbf{r}(t)$ is the radius vector of the scattering element. If the amplitude $A(t)$ is assumed to be slowly varying during the time about the inverse Doppler frequencies of the signal, we readily obtain that

$$S(\omega, t) = P(t) [\delta(\omega - 2\mathbf{k}_e \mathbf{V}) + \delta(\omega + 2\mathbf{k}_e \mathbf{V})]/2. \quad (\text{A8})$$

Here, $\mathbf{V} = d\mathbf{r}/dt$ is the scattering-element velocity on the sea surface.

When deriving Eq. (A8), it was assumed for simplicity that the radar-antenna directional pattern is sufficiently narrow and the irradiated-spot size on the sea surface is about the spatial-coherence scale of the scattering ripples or smaller. In this case, it can be assumed that all the scatterers within the spot limits move with the same velocity. Allowance for the differences in the phases of the waves scattered by different surface regions within the spot limits due to the differences among the scattering-element velocities leads to a certain blurring of the instantaneous spectrum which is insignificant during finding its barycenter, i.e., the Doppler shift.

It follows from Eqs. (A1) and (A8) that the Doppler shift

$$F_I(t) = \pi k_e \sin(\theta) [C_s + V_m + U_{\text{orb}}(t)]. \quad (\text{A9})$$

Equation (A9) assumes that the scattering-element velocity is composed of the scattering-wave phase velocity C_s , the mean stream velocity V_m (including the wind drift), and the orbital velocity $U_{\text{orb}}(t)$ of the long-wave field, where θ is the electromagnetic-wave incidence angle. The terms proportional to the highest degrees of the small tilts of the long waves are neglected in Eq. (A9). Then the average Doppler shift

$$F_I = \pi k_e \sin(\theta) (C_s + V_m) \quad (\text{A10})$$

of the instantaneous spectrum is determined by the phase velocity of the Bragg wave and the mean stream velocity.

The expression for the Doppler shift of the average spectrum is readily obtained from Eqs. (A2), (A4), (A8), and (A9). In the case of observation along the long-wave propagation direction, i.e., downwind measurements, we have

$$F_A = \bar{F}_I + \frac{2k_e}{\pi} \text{Re} \int_0^\infty m(\Omega) \frac{U(\Omega)}{C(\Omega)} \bar{U}^*(\Omega) (\sin \theta + i \cos \theta) \, d\Omega, \quad (\text{A11})$$

where

$$\bar{U}(\Omega) = \int \frac{U(\Omega_1) \sin[(\Omega - \Omega_1) T/2]}{(\Omega - \Omega_1) T/2} \, d\Omega_1 \approx U(\Omega) 4\pi/T$$

is the amplitude of the velocities of the long surface wave in the band about $4\pi/T$ near the frequency Ω .

Therefore, the difference between the Doppler shifts F_A and F_I is determined by the radar-signal modulation degree and can be pronounced in the presence of intense long waves.

REFERENCES

1. A. S. Monin and V. P. Krasitskii, *Phenomena on the Ocean Surface* [in Russian], Gidrometeoizdat, Leningrad (1985).
2. S. V. Viktorov and L. M. Mitnik, eds., *Radar Observations of the Earth's Surface from Space* [in Russian], Gidrometeoizdat, Leningrad (1990).
3. M. G. Bulatov, Yu. A. Kravtsov, O. Yu. Lavrova, et al., *Physics — Uspekhi*, **46**, No. 1, 63 (2003).
4. O. Yu. Lavrova, A. G. Kostyanoy, S. A. Lebedev, et al., *Complex Satellite Monitoring of the Seas of Russia* [in Russian], Inst. Space Res., Moscow (2011).
5. B. Chapron, F. Collard, and F. Ardhuin, *J. Geophys. Res.*, **110**, C07008 (2005).
6. A. A. Mouche, F. Collard, B. Chapron, et al., *IEEE Trans. Geosci. Remote Sensing*, **50**, No. 7, 2901 (2012).
7. F. G. Bass and I. M. Fuks, *Wave Scattering from Statistically Rough Surfaces*, Pergamon Press, Oxford (1979).
8. S. M. Rytov, Yu. A. Kravtsov, and V. I. Tatarskii, *Principles of Statistical Radiophysics*, Springer-Verlag, Berlin (1989).
9. M. S. Longuet-Higgins, *J. Fluid Mech.*, **16**, 138 (1963).
10. K. D. Ruvinskii, F. I. Feldstein, and G. I. Freidman, *J. Fluid Mech.*, **230**, 339 (1991).
11. S. A. Ermakov, K. D. Ruvinskii, S. G. Salashin, and G. I. Freidman, *Izv. Akad. Nauk SSSR, Fiz. Atmos. Okeana*, **22**, No. 10, 1072 (1986).
12. M. Longuet-Higgins, *J. Fluid Mech.*, **301**, 79 (1995).
13. W. J. Plant, W. C. Keller, V. Hesany, et al., *J. Geophys. Res.*, **104**, No. 2, 3243 (1999).
14. M. Gade, W. Alpers, S. A. Ermakov, et al., *J. Geophys. Res.*, **103**, No. 10, 21697 (1998).
15. S. A. Ermakov, I. A. Kapustin, and I. A. Sergievskaya, *Bull. Rus. Acad. Sci. Phys.*, **74**, No. 12, 1695 (2010).
16. S. A. Ermakov, I. A. Kapustin, and I. A. Sergievskaya, *Radiophys. Quantum Electron.*, **55**, No. 7, 453 (2012).
17. V. Kudryavtsev, D. Hauser, G. Caudal, and B. Chapron, *J. Geophys. Res.*, **108**, No. 3, 8054 (2003).
18. V. Kudryavtsev, D. Hauser, G. Caudal, and B. Chapron, *J. Geophys. Res.*, **108**, No. 3, 1 (2003).
19. V. Kudryavtsev, D. Akimov, J. Johannessen, and B. Chapron, *J. Geophys. Res.*, **110**, 07016 (2005).
20. T. Hara and W. J. Plant, *J. Geophys. Res.*, **99**, No. 5, 9767 (1994).
21. S. A. Ermakov, I. A. Sergievskaya, and Yu. B. Shchegolkov, *Radiophys. Quantum Electron.*, **25**, No. 12, 942 (2002).
22. S. A. Ermakov, I. A. Sergievskaya, E. M. Zuykova, and Yu. B. Shchegolkov, *Izvestiya, Atmos. Ocean. Phys.*, **40**, No. 1, 91 (2004).
23. V. N. Kudryavtsev, V. K. Makin, and B. Chapron, *J. Geophys. Res.*, **104**, 7625 (1999).
24. A. Rosenberg, M. Ritter, W. K. Melville, et al., *IEEE Trans. Geosci. Remote Sensing*, **37**, No. 2, 1052 (1999).
25. P. H. Y. Lee, J. D. Barter, K. L. Beach, et al., *J. Geophys. Res.*, **100**, No. 2, 2591 (1995).
26. Yu. A. Kravtsov, M. I. Mityagina, and A. N. Churyumov, *Radiophys. Quantum Electron.*, **42**, No. 3, 216 (1999).
27. W. J. Plant, *J. Geophys. Res.*, **87**, No. 1, 1961 (1982).